

RI 8997

RI	8997
-----------	-------------

PLEASE DO NOT REMOVE FROM LIBRARY

Bureau of Mines Report of Investigations/1985

Utilization of Simulated Coal Gases for Reducing Iron Oxide Pellets

By Larry A. Haas, John C. Nigro, and Robert K. Zahl



UNITED STATES DEPARTMENT OF THE INTERIOR



Report of Investigations 8997

Utilization of Simulated Coal Gases for Reducing Iron Oxide Pellets

By Larry A. Haas, John C. Nigro, and Robert K. Zahl



UNITED STATES DEPARTMENT OF THE INTERIOR
Donald Paul Hodel, Secretary

BUREAU OF MINES
Robert C. Horton, Director

Library of Congress Cataloging in Publication Data:

Haas, L. A. (Larry A.)

Utilization of simulated coal gases for reducing iron oxide pellets.

(Report of investigations / United States Department of the Interior, Bureau of Mines ; 8997)

Bibliography: p. 14.

Supt. of Docs. no.: I 28.23: 8997.

1. Iron--Metallurgy. 2. Iron oxides. 3. Reduction, Chemical. 4. Gas. I. Nigro, John C. II. Zahl, Robert K. III. Title. IV. Series: Report of investigations (United States, Bureau of Mines) ; 8997.

TN23.U43 [TN707] 622s [669'.14] 85-600202

CONTENTS

	<u>Page</u>
Abstract.....	1
Introduction.....	2
Acknowledgments.....	3
Experimental work.....	3
Materials.....	3
Procedure.....	3
Results and discussion.....	4
Single-reductant gas mixtures.....	4
Simulated reformed and coal-gas mixtures.....	9
Evaluation of reduced pellets.....	12
Conclusions.....	13
References.....	14

ILLUSTRATIONS

1. Experimental equipment used in reduction studies of iron oxide pellets....	3
2. Influence of gas flow rates on percent reduction with 100 pct H ₂ at 900° C	4
3. Comparison of reduction-rate data using various normalized reduction functions.....	5
4. Arrhenius plots with 100 pct H ₂ , CO, or CH ₄	5
5. Plot of logarithm of reductant pressure and reduction rate at 900° C.....	6
6. Influence of CO ₂ and CO on reduction at 900° C.....	7
7. Equilibrium diagram of iron in presence of various gases.....	7
8. Influence of water vapor and CO ₂ on reduction rate constant at 900° C.....	8
9. Influence of water vapor in H ₂ on reduction at 900° C.....	8
10. Dependence of calculated and experimental reduction rate constants on gas composition and temperature.....	11
11. Dependence of the 90-pct reduction time on type of reducing gas and temperature.....	12
12. Pellet pore size distribution before and after reduction.....	13

TABLES

1. Partial analyses of actual and simulated reducing-gas mixtures.....	2
2. Partial chemical analyses of fired iron oxide pellets before reduction....	3
3. Chemical and physical properties of reduced iron oxide pellets.....	10

UNIT OF MEASURE ABBREVIATIONS USED IN THIS REPORT

atm	atmosphere	kcal/mol	kilocalorie per mole
Btu	British thermal unit	kg	kilogram
°C	degree Celsius	lb	pound
cm	centimeter	μm	micrometer
g	gram	mm	millimeter
g/cm ³	gram per cubic centimeter	min	minute
h	hour	pct	percent
in	inch	scf	standard cubic foot
K	kelvin	SLM	standard liter per minute

UTILIZATION OF SIMULATED COAL GASES FOR REDUCING IRON OXIDE PELLETS

By Larry A. Haas,¹ John C. Nigro,² and Robert K. Zahl³

ABSTRACT

The Bureau of Mines is investigating the use of complex gas mixtures, such as would be produced by coal gasification, for reducing iron oxide pellets. A semiempirical model was developed to predict a priori the reduction rate of an iron oxide pellet in a laboratory tube furnace with simulated coal gases at a total pressure of 1 atm. The model uses partial pressures of H₂, CO, CO₂, CH₄ (methane), water vapor, and a temperature-dependent term to predict the rate of reaction. The reduction rate (weight loss per unit of time) was determined with a thermogravimetric apparatus (TGA) in the temperature range of 800° to 1,100° C. The ranking of the reductants, in order of decreasing reducing potential, is H₂, CO, and CH₄ at temperatures between 800° and 1,000° C; however, CH₄ became a better reductant than CO at 1,100° C. Water vapor did not decrease the reduction rate as much as did CO₂. Carbon deposition was observed at temperatures below 1,000° C with gas mixtures with high CO and low H₂ concentrations. With low-Btu gas at 900° C, over 90 pct of the iron oxide was reduced to iron in less than 3 h. This compares with a reduction time of 1.5 h with medium-Btu gas and 1 h with reformed natural gases.

¹Research chemist.

²Supervisory physical scientist.

³Supervisory metallurgist.

Twin Cities Research Center, Bureau of Mines, Minneapolis, MN.

INTRODUCTION

The Bureau of Mines, as part of its mission to investigate alternative technologies for processing domestic iron ores, conducted research to determine the reducibility of iron oxide pellets using different gaseous coal-based reductants. The most successful commercial direct-reduced iron (DRI) processes are natural gas based (10).⁴ However, reductants made from natural gas and liquid fuels are becoming more costly, and their stable domestic supply for such applications is limited. To allow commercialization of DRI processes in the United States, information must be obtained so that coal-based DRI processes can be developed.

During the past several years, the Bureau of Mines (at its Twin Cities Research Center) has operated a single-stage, fixed-bed, air-blown gasifier with bituminous, subbituminous, and lignite coals (16) to generate a low-Btu gas for metallurgical application. The H₂ and CO contents of this gas are lower than those of the gas produced by oxygen-blown gasifiers (table 1). For purposes of

comparison, the gas compositions from other gasifiers and other sources are also shown in table 1, along with gas codes and some definitions of the terms used in this report.

Considerable research has been conducted on the reduction kinetics of iron oxides with single-component gas reductants (6), but very few data are available regarding experimental reduction kinetics using complex gas mixtures such as would be produced by coal gasification. A report (11) was published recently on the reduction of iron oxide pellets with low-Btu gas, but it mainly dealt with the inhibiting influence of hydrogen sulfide on reduction.

Since only very limited data are available on the iron oxide reducibility potential of coal (producer) gases, a research program was initiated to develop an experimental model whereby the reduction rate could be predicted from the gas composition and temperature. Reduction kinetic data were obtained first with single-reductant gas mixtures and then with more complex multireductant gas mixtures. In some tests, the pellet compression strengths and porosities were also evaluated before and after reduction.

⁴Underlined numbers in parentheses refer to items in the list of references at the end of this report.

TABLE 1. - Partial analyses of actual and simulated reducing-gas mixtures

Gas code	Type of gas mixture	Chemical analysis, pct								Reference
		H ₂	CO	CH ₄	CO ₂	H ₂ O	H ₂ +CO+CH ₄	CO ₂ +H ₂ O	N ₂	
ACTUAL FURNACE GASES										
LAG..	Lignite air gasifier.....	20	27	2	7	21	49	28	23	16
COG..	Coal oxygen gasifier.....	33	59	1	7	1	93	8	0	2
CCO..	Coal-CO ₂ acceptor.....	59	15	14	9	1	88	10	2	4
RNGR.	Reformed natural gas (recycled)	49	47	1	1	2	97	3	0	4
RNG..	Reformed natural gas.....	71	23	1	1	4	95	5	0	4
SIMULATED COMPLEX GAS MIXTURES										
L-Btu	Low-Btu ¹	20	27	2	7	0	49	7	44	16
M-Btu	Medium-Btu ¹	37	47	3	13	0	87	13	4	2
RF-1.	Reformed gas-1.....	50	48	1	1	0	99	1	0	4
RF-2.	Reformed gas-2.....	55	35	3	7	0	93	7	0	4
RF-3.	Reformed gas-3.....	73	13	5	9	0	91	9	0	4

¹Low-Btu = 85 to 200 Btu/scf; medium-Btu = 260 to 325 Btu/scf (2).

ACKNOWLEDGMENTS

The authors wish to express their gratitude to Jeff A. Aldinger for his help with the reduction tests, and Edward J. Helmueller, who determined the physical

properties of the pellets. Both of these were students employed at the Twin Cities Research Center during the summer of 1984.

EXPERIMENTAL WORK

MATERIALS

The iron oxide pellets used in this research were commercially produced from a magnetite concentrate. The pellets were sized to minus 1/2 in (12.7 mm) and plus 7/16 in (11.1 mm). Several hundred sized pellets were further classified by weight in the range of 3.1 to 3.4 g. Typical analyses of the pellets are shown in table 2. The percent oxygen was 28.5 as determined by the weight loss at 100-pct reduction; in this report, it was assumed that the weight loss was proportional to the percent reduction. The pellet strength of 20 pellets before reduction was 293 ± 138 lb (133 ± 63 kg); the first value is the mean value, and the second value is the standard deviation. Some of the other pellet properties before reduction follow: porosity = 24 ± 4 pct, and pore diameter at 50 pct pore volume = 4.0 ± 0.9 μ m. The porosity value only includes the surface-connected open pores and those accessible by the mercury porosimeter technique. The true density of the pellet, ground to 100 pct minus 325 mesh, was 4.9 ± 0.2 g/cm³.

TABLE 2. - Percentage chemical analyses of fired iron oxide pellets before reduction

Chemical	Pct	Chemical	Pct
Fe _T ¹	66.3	Na ₂ O.....	0.03
Fe ²⁺3	K ₂ O.....	.02
SiO ₂	3.0	TiO ₂8
Al ₂ O ₃6	C.....	.2
CaO.....	.9	P.....	.12
MgO.....	.3	S.....	.01
MnO ₂06		

¹Total iron content.

PROCEDURE

For each test, one iron oxide pellet was selected at random from a large batch of indurated pellets. Before and after each test, the pellet diameter and weight was determined. During the test, the pellet was held in a platinum wire-mesh basket (fig. 1) suspended with a platinum chain from the left pan of an automatic recording balance (sensitivity and reproducibility better than ± 0.002 g).

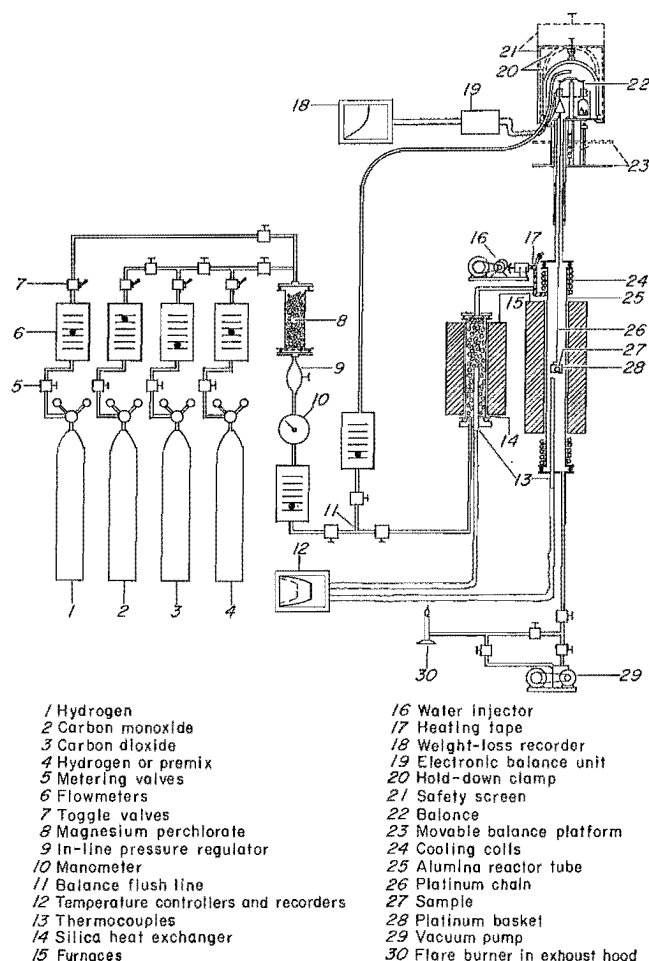


FIGURE 1. - Experimental equipment used in reduction studies of iron oxide pellets.

Chemically pure (>99.9 pct) single-component or premixed gases were metered into the gas preheater and then to the thermogravimetric analysis apparatus. The furnace pressure was 1 atm and the total flow rate was 1.5 SLM, unless otherwise stated. Ten percent of this gas was not preheated but was used to flush the bell jar before the gas entered the pellet reactor chamber (80-cm-long, 5-cm-diam alumina tube). Before the heat was turned on, the reactor chamber and balance unit were evacuated to 0.1 atm and then backfilled with nitrogen. This procedure was repeated three times. The reactor was heated in 1 SLM nitrogen gas

to within 5° C of the desired operating temperature before the balance platform was lowered to place the pellet in the 10-cm-long hot zone. Five minutes after the pellet was lowered into the hot zone, the nitrogen flow was shut off and the reducing gas flow was started. Unless otherwise stated, the reducing-gas flow was maintained until no further weight loss was observed, or for a maximum of 4 h. After this time, the nitrogen flow was turned on and the pellet was raised into the cold zone. The power to the furnace then was turned off, and, after the furnace was flushed for 2 h, the nitrogen gas lines closed.

RESULTS AND DISCUSSION

SINGLE-REDUCTANT GAS MIXTURES

The reduction rates were first determined with the single-gas reductants (100 pct H₂, CO, or CH₄). The temperature of 900° C was selected for the baseline tests. With the 100 pct H₂ gas, the reduction rate increased with the increasing flow rates from 0.3 to 1.5 SLM, but between 1.5 and 4.4 SLM, very little change in the reduction rate was observed (fig. 2). With 100 pct CO or CH₄, a flow of 0.8 SLM was fast enough to reach the critical flow rate. In the

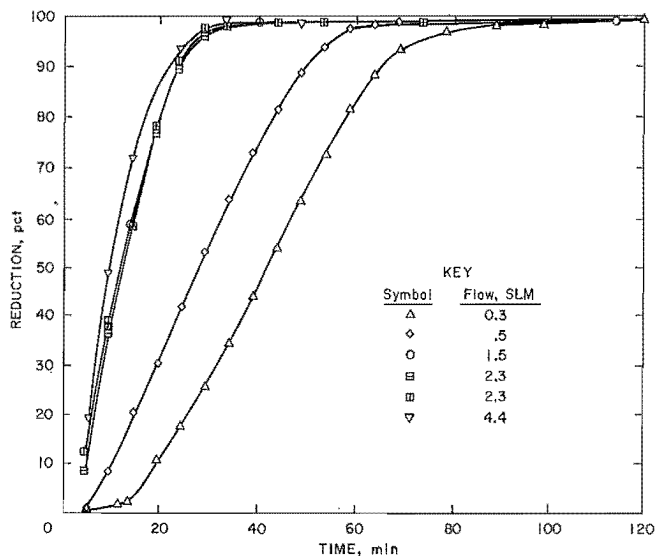


FIGURE 2. - Influence of gas flow rates on percent reduction with 100 pct H₂ at 900° C.

tests conducted at temperatures higher than 900° C, the gas flows were 2.3 SLM with 100 pct H₂ and 1.5 SLM with all the other gases.

The reduction data with 100 pct H₂ gas at 900° C were used to determine the best equation for subsequent comparison of different reductants. Hydrogen was chosen as the baseline reductant because it was expected to be the best reductant, and one would expect the least number of complicating side reactions. The normalized weight-loss (percent-reduction) data were expressed in various forms using different equations; the values from the left side of the equation (y) versus time are shown in figure 3. Straight-line regression correlations were calculated for reduction values ranging from 10 to 90 pct and are shown as dashed lines. The weight-loss data obtained on the strip-chart recorder can be expressed by equation 1:

$$R/100 = A(t) + B, \quad (1)$$

where R is the percent reduction, A is the slope, t is the time in minutes, and B is a constant. A low correlation coefficient of 0.940 was obtained with this equation. A much higher correlation coefficient of 0.993 was obtained using equation 2:

$$[1 - (1-R/100)^{1/3}] = k_e (t) + C, \quad (2)$$

where k_e is the experimental rate constant in reciprocal minutes, and C is a constant. The theoretical basis of equation 2 is the assumption that the chemical reaction at the receding interfacial shell surface is the rate-controlling mechanism (15, 18). If the rate-controlling mechanism was solely the gaseous diffusion through the product layer, then the time dependence of the degree of reduction of a sphere should follow the parabolic law (17), which can be expressed by equation 3:

$$\begin{aligned} 1/2 - R/300 - 1/2 (1-R/100)^{2/3} \\ = k' (t) + D, \end{aligned} \quad (3)$$

where k' is the parabolic rate constant, and D is a constant. Equation 3 produced a lower correlation coefficient (0.986) than did equation 2. Turkogan (19) reported that the rate-controlling step depends essentially on the uniform internal reaction on the pore walls, and they obtained a good fit with equation 4:

$$\log (1 - R/100) = -k'' (t) + E, \quad (4)$$

where k'' is the first-order rate constant in reciprocal minutes, and E is a constant. With equation 4, the correlation coefficient was 0.987.

The highest correlation coefficient was obtained with equation 2, and therefore this equation was used to compare the results in this report. Figure 3 also shows that this equation fits the data better than the other equations even up to about 95-pct reduction.

With 100 pct H_2 , CO , or CH_4 gas, the dependence of the rate constants (k_e) on temperature was determined at 800°, 900°, 1,000°, and 1,100° C; the results are shown in the Arrhenius plot (fig. 4). The apparent activation energies were calculated using the following equation:

$$\log k_e = \frac{\Delta H^*}{4.575} (10^3/T) + F, \quad (5)$$

where ΔH^* is the apparent activation energy in kilocalories per mol, T is the temperature in kelvins, and F is a constant. The influence of temperature on

the activation energies was calculated by the least-squares regression method, and the values for 100 pct H_2 , CO , and CH_4 were 14.2, 13.7, and 40.6 kcal/mol,

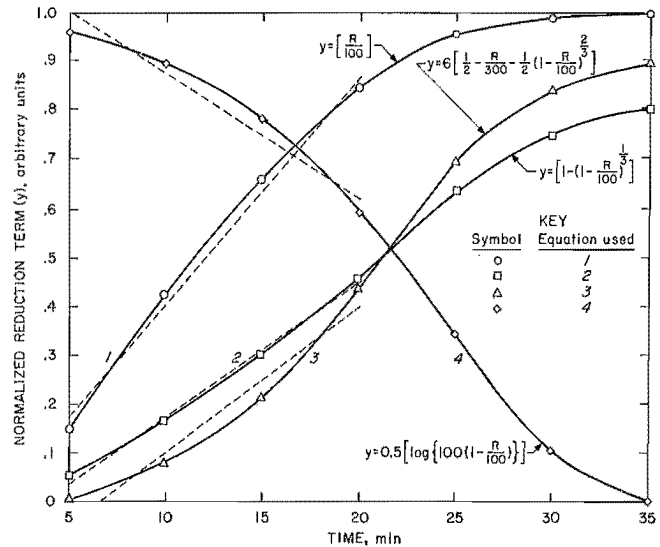


FIGURE 3. - Comparison of reduction-rate data using various normalized reduction functions (the best fit straight lines between 10- and 90-pct reduction are shown as dashed lines).

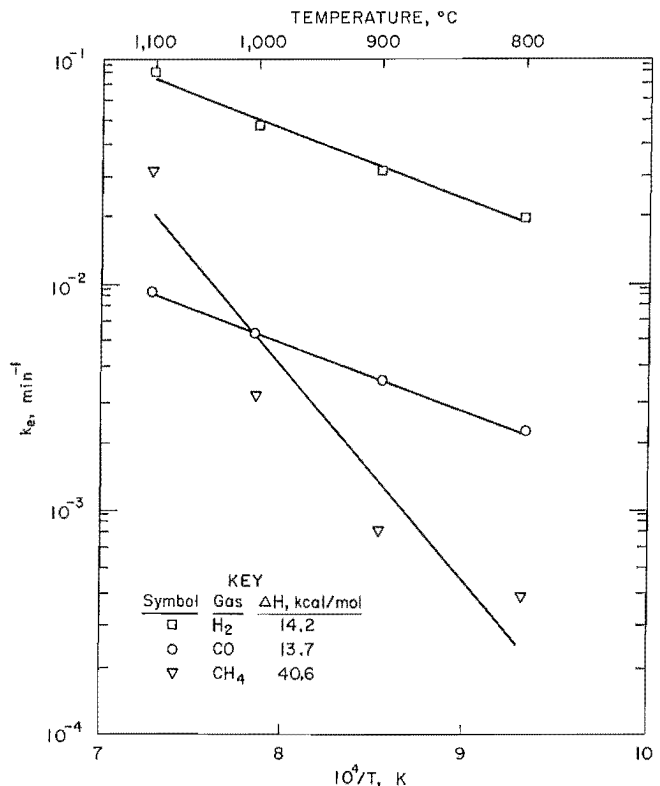


FIGURE 4. - Arrhenius plots with 100 pct H_2 , CO , or CH_4 .

respectively. These values are in fair agreement with those of other investigators. Kurgina (13) reported values of 14.5 and 17.3 kcal/mol for H₂ and CO, respectively. Hansen (6) obtained values of 10.8 kcal/mol with H₂ and 11.5 kcal/mol with CO using a red iron ore from Alabama. However, earlier work by his group (8) reported a value of 15.3 kcal/mol with H₂ using a different iron ore from Minnesota. The activation energy with CH₄ was considerably higher, but Mazhenov (14) also reported a high value (43.0 kcal/mol).

The results in figure 4 show that 100 pct H₂ is a much better reductant than is 100 pct CO, which is in agreement with other investigators (8, 12). One-hundred-percent CH₄ is a poor reductant at 800° C, but at 1,100° C, it is between CO and H₂.

Reduction rates were then determined with reductants diluted with N₂ at 900° C, and the total flow was kept constant at 2.3 SLM. Figure 5 shows the curves for the logarithm of the reductant partial pressure versus logarithm of the reduction rate. Fairly linear curves were obtained and the lines were defined by equation 6:

$$\log k_e = z \log P_r + G, \quad (6)$$

where z is the exponent of the reductant partial pressure, P_r is the partial pressure of the reductant in atmospheres, and G is a constant. The values for z with H₂, CO, and CH₄ were 1.60, 0.59, and 1.80, respectively.

Different partial pressures of CO and H₂ were also obtained by dilution with CO₂ and water vapor, respectively. Water vapor and CO₂ are not only diluents but also oxidants, which can cause the reduction reactions to reverse. Al-Kahtany (1) reported that when oxidants are present with reductants, a mathematical function of the partial pressure of the oxidant must be subtracted from the partial pressure of the reductant for determining the reaction rate constants.

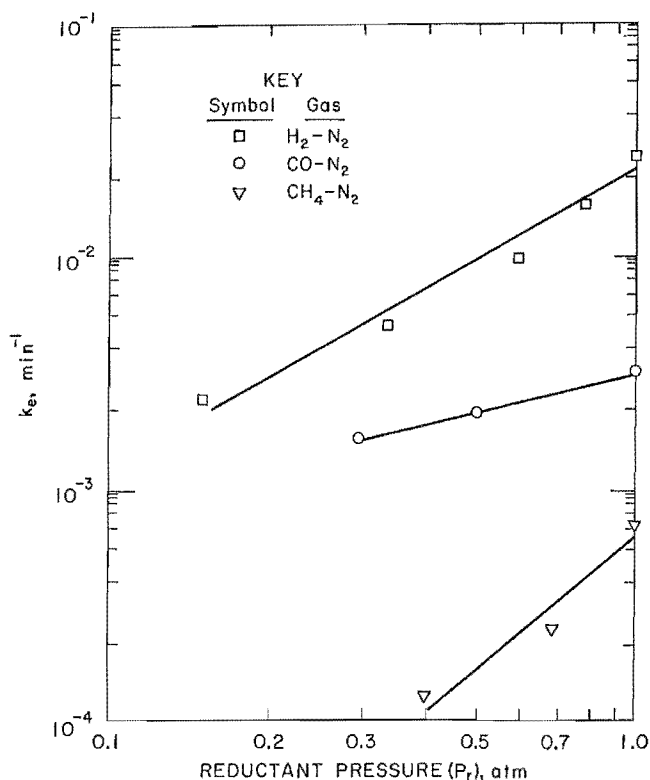


FIGURE 5. - Plot of logarithm of reductant pressure and reduction rate at 900° C.

The results obtained by adding CO₂ to CO are shown in figure 6. It can be seen from these results that the two duplicate CO tests are similar, but increasing the oxidant pressure (P_o) retards the reduction rates. With 40 pct CO₂ in CO, the curve levels off at about 30-pct reduction. The conversion from hematite to wustite (Fe_xO, where x ranges between 0.83 and 0.95) corresponds to about a 30-pct reduction; with this gas mixture at 900° C, the reduction to metallic iron does not seem to occur. These results are in agreement with thermodynamic data shown in figure 7. The reduction rate constants for the CO₂ additions to CO gas mixtures are plotted in figure 8. The calculated CO-CO₂ rate curve indicates that a fairly good fit was obtained with equation 7:

$$k_{\text{CO-CO}_2} = 0.18 \left[7.0 (P_{\text{CO}})^{0.59} - \frac{P_{\text{CO}_2}}{0.01 + 0.19 P_{\text{CO}_2}} \right] e^{-13,700/RT}, \quad (7)$$

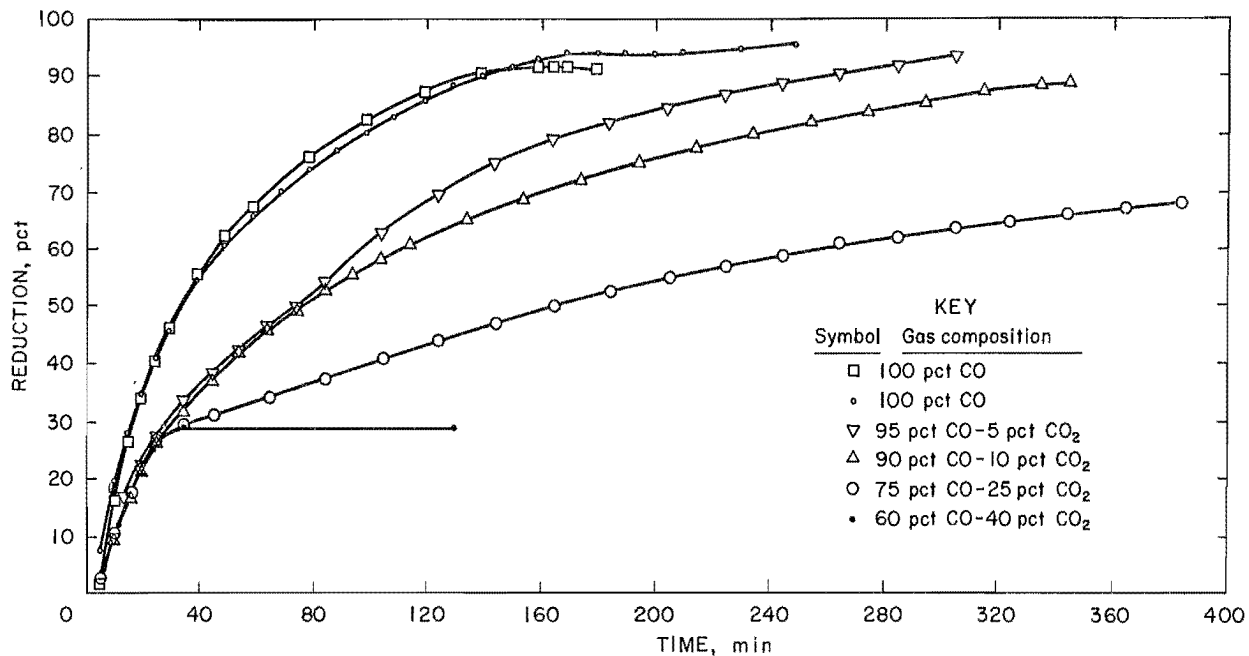


FIGURE 6. - Influence of CO₂ and CO on reduction at 900° C.

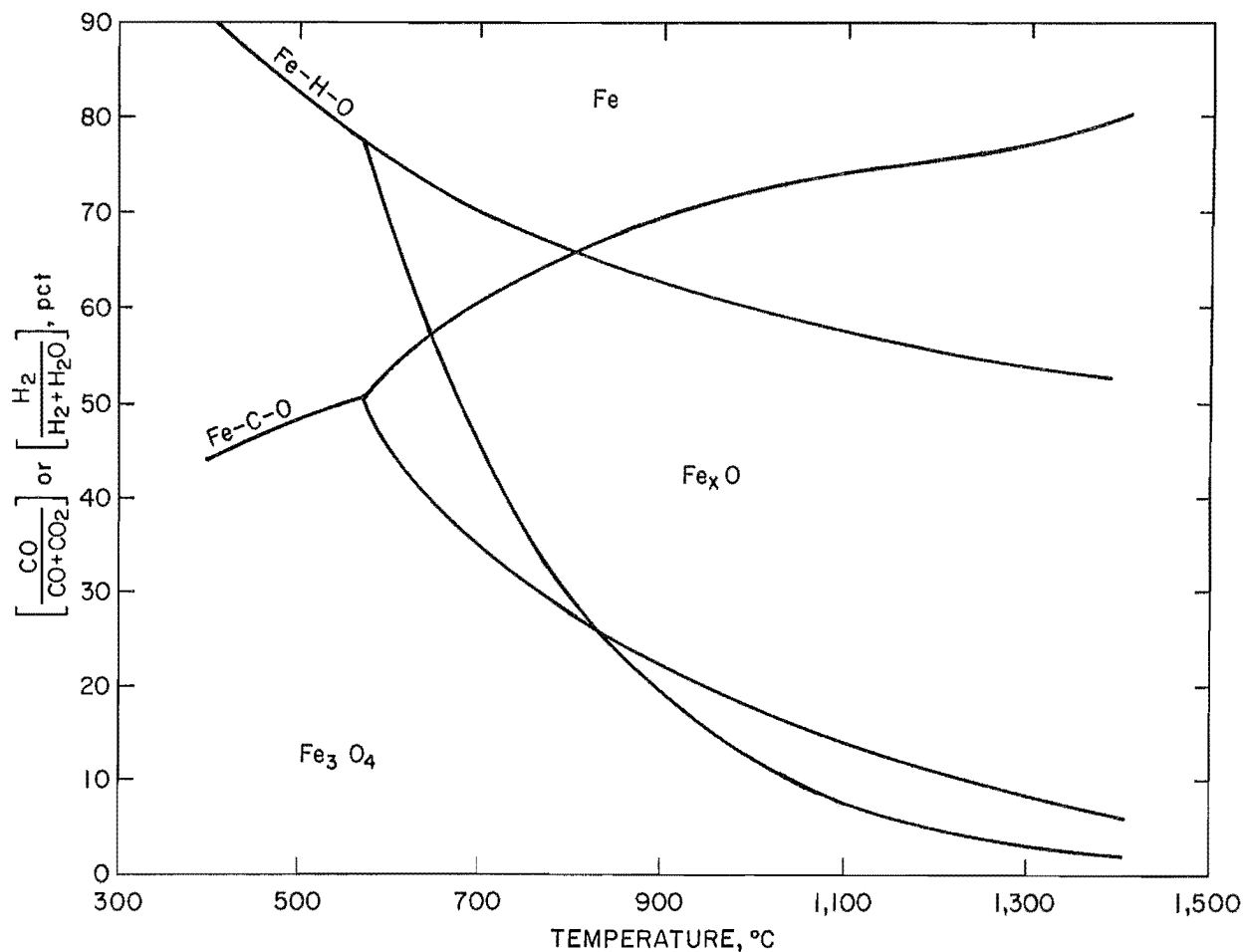


FIGURE 7. - Equilibrium diagram of iron in presence of various gases (7).

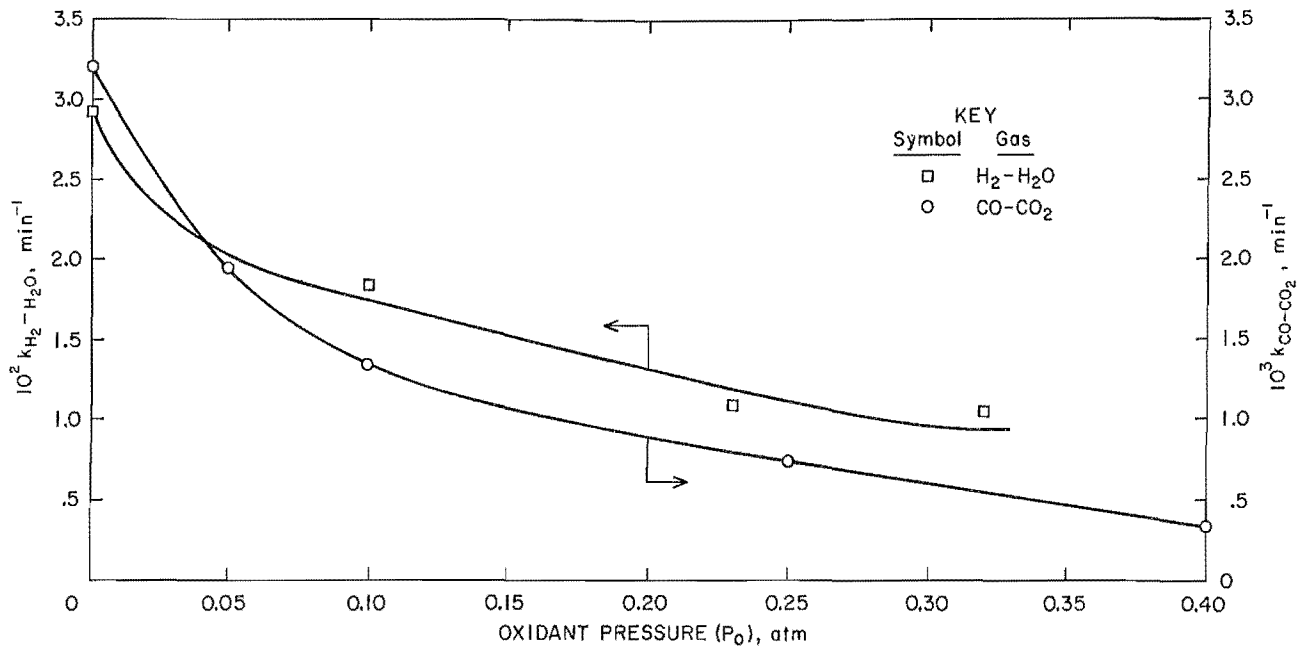


FIGURE 8. - Influence of water vapor and CO₂ on reduction rate constant at 900° C.

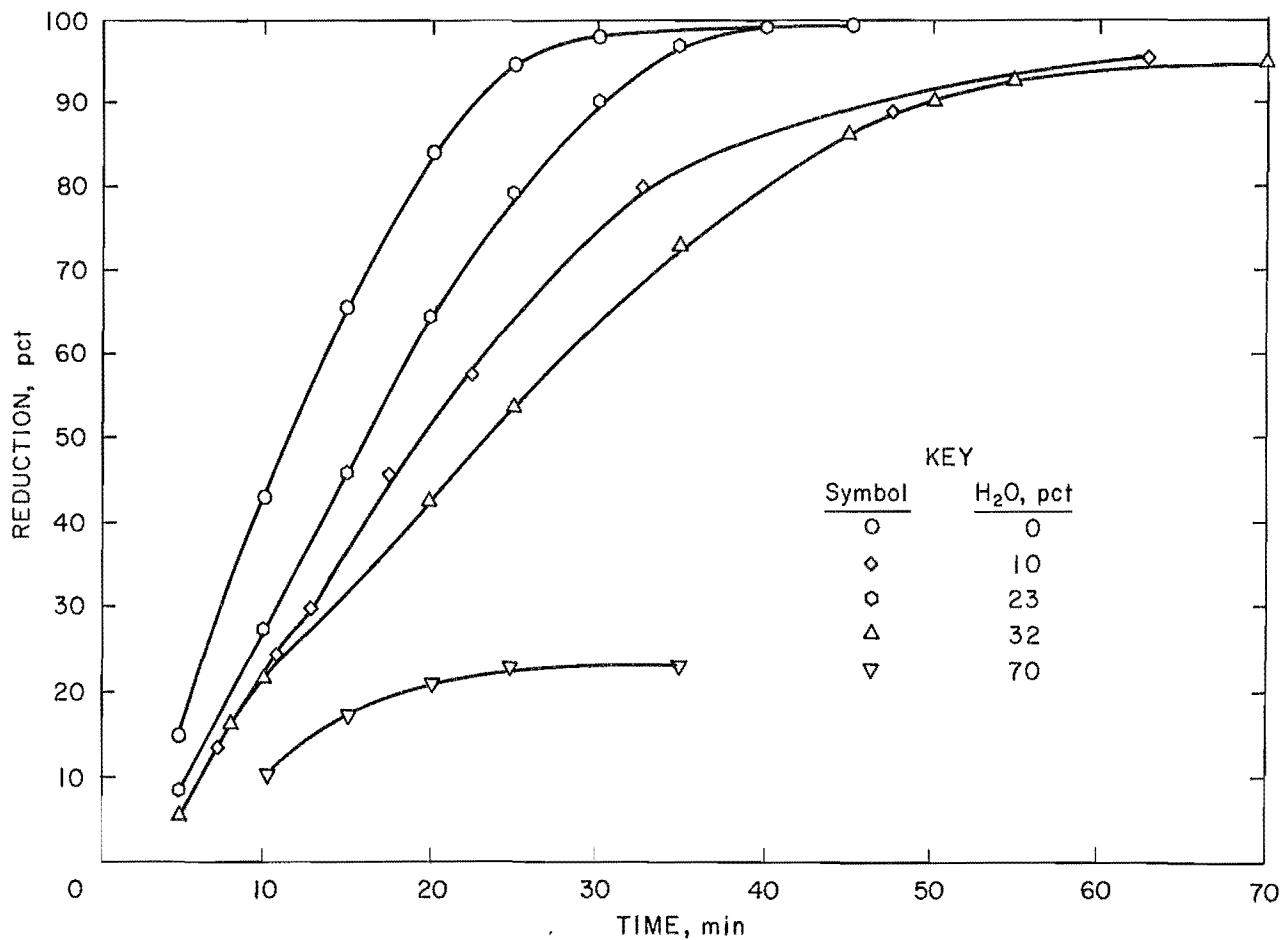


FIGURE 9. - Influence of water vapor in H₂ on reduction at 900° C.

where $k_{\text{CO-CO}_2}$ is the rate constant for CO-CO₂ reduction reaction, and P_{CO_2} is the partial pressure of CO₂ in atmospheres. This semiempirical equation was obtained by trying different constants until a fairly good fit was obtained. The deviations of the experimental rates from the values calculated from this equation were 5 pct or less in the range of 0 to 25 pct CO₂. In developing this equation, the assumptions were made that the activation energy and the exponent for the partial pressure of the reductant did not change as the oxidant content was increased. The assumption was also made that the constants were independent of temperature in the range from 800° to 1,100° C. No conclusive mechanism is

implied by the magnitude of these constants and the form of this equation.

The effect of water vapor in H₂ on the iron oxide reduction rate at 900° C was also determined (fig. 9). It is evident from these results that water retards the reduction rate. With 70 pct water vapor, the reduction leveled off below 30 pct. This suggests that the reduction stopped at wustite and did not proceed to metallic iron, which was expected from the data shown in figure 7. The reduction rate constants were calculated with water vapor added to H₂, and the data were plotted in figure 8. The calculated H₂-H₂O curve indicates that a fairly good fit was obtained with equation 8:

$$k_{\text{H}_2\text{-H}_2\text{O}} = 0.22 \left[60(P_{\text{H}_2})^{1.6} - \frac{P_{\text{H}_2\text{O}}}{0.0005 + 0.06 P_{\text{H}_2\text{O}}} \right] e^{-14,200/RT}, \quad (8)$$

where $k_{\text{H}_2\text{-H}_2\text{O}}$ is the rate constant for the H₂-H₂O reduction reaction, and $P_{\text{H}_2\text{O}}$ is the partial pressure of water in atmospheres. The deviations of the experimental rates from the values calculated from this semiempirical equation were 6 pct or less in the range of 0 to 23 pct H₂O.

SIMULATED REFORMED AND COAL GAS MIXTURES

The tests discussed earlier in this report were conducted with gases containing

only one or two components, but commercial processes use more complex gas mixtures containing predominantly H₂, CO, CH₄, CO₂, and water vapor. (See table 1.) Several cylinders of simulated complex gas mixtures were purchased for determining the reduction rates at various temperatures. Table 3 shows the experimental and calculated rate constants for both the single-reductant and complex gas mixtures. By combining the previously developed equations and data, the calculated rate constants (k_c) for the complex gases were obtained by using equation 9:

$$\begin{aligned} k_c = & 0.22 \left[60(P_{\text{H}_2})^{1.6} - \frac{P_{\text{H}_2\text{O}}}{0.0005 + 0.06 P_{\text{H}_2\text{O}}} \right] e^{-14,200/RT} \\ & + 0.18 \left[7.0 (P_{\text{CO}})^{0.59} - \frac{P_{\text{CO}_2}}{0.01 + 0.19 P_{\text{CO}_2}} \right] e^{-13,700/RT} \\ & + 2.3 \times 10^4 \left[(P_{\text{CH}_4})^{1.8} \right] e^{-40,600/RT}. \end{aligned} \quad (9)$$

TABLE 3. - Chemical and physical properties of reduced iron oxide pellets¹

Gas temp., °C	Partial chemical analysis, pct		Carbon, pct	Swelling ² (100 V _f /V _i), pct	Strength, ³ kg	r ₄₀ , ⁴ pct/min	Reaction rate, min		Time, min ⁵		
	Fe _T , Fe°	100 Fe°/Fe _T					10 ² k _e	10 ² k _c	t ₉₀	t _{max}	
H ₂ :											
800	92.7	87.1	94	0.1	10	97	4.2	1.83	1.72	30	85
900	92.5	89.1	96	.1	ND	59	5.2	2.95	3.03	25	35
1,000	92.7	91.3	98	ND	13	41	8.4	4.61	4.89	15	20
1,100	90.0	88.3	98	.1	22	41	16.8	8.01	7.36	8	10
CO:											
800	68.1	56.3	83	5.3	ND	ND	.5	.22	.21	ND	160
900	90.1	84.8	94	2.2	10	100	1.1	.35	.35	140	140
1,000	90.8	88.4	97	2.4	10	97	1.5	.55	.56	90	135
1,100	90.8	87.5	96	1.0	32	43	2.3	.90	.83	45	80
L-Btu:											
800	92.4	87.2	94	.2	ND	ND	.1	.25	.14	215	240
900	91.1	85.4	94	.1	21	ND	.4	.33	.24	155	240
1,000	91.1	85.9	94	.1	ND	ND	.9	.39	.39	132	240
1,100	90.8	87.6	96	.2	30	23	2.1	.83	.59	55	75
M-Btu:											
800	90.4	83.0	92	.5	ND	ND	1.1	.48	.37	115	200
900	91.5	85.0	93	.4	ND	ND	1.2	.51	.66	95	140
1,000	91.3	86.3	95	.3	ND	ND	1.5	.77	1.06	70	85
1,100	93.0	88.3	95	.1	ND	ND	2.8	1.63	1.59	35	45
RF-1:											
800	89.4	77.1	86	1.6	ND	ND	1.6	.67	.67	90	85
900	93.0	86.4	93	1.2	ND	ND	2.9	1.22	1.17	50	75
1,000	93.7	89.8	96	.8	ND	ND	ND	1.68	1.89	30	40
1,100	92.3	92.1	100	.2	22	ND	5.1	2.55	2.83	20	30
RF-2:											
800	91.5	88.4	97	.3	10	104	2.0	.88	.69	65	90
900	90.6	85.9	95	.4	10	63	3.1	1.31	1.21	55	80
1,000	92.3	89.6	97	.3	10	59	4.5	2.20	1.95	25	60
1,100	91.7	88.8	97	.2	16	18	7.5	3.36	2.94	15	20
RF-3:											
800	91.7	89.6	98	.1	10	ND	2.2	.87	1.03	60	125
900	89.0	85.7	96	.1	10	ND	4.2	1.66	1.81	35	85
1,000	89.2	85.9	96	.2	10	50	4.4	2.33	2.93	25	65
1,100	91.2	88.8	97	.2	26	23	6.7	4.59	4.42	10	15
CH ₄ :											
800	73.4	38.2	52	10.3	106	50	ND	.04	.02	ND	240
900	67.6	64.9	96	26.8	106	4	ND	.08	.07	ND	240
1,000	66.0	64.3	97	26.9	101	4	ND	.30	.25	ND	⁶ 80
1,100	63.9	63.0	99	29.0	ND	ND	5.2	2.99	.81	20	⁶ 25

ND Not determined.

¹Reduction time was 4 h or until a maximum weight loss was observed.

²Swelling was defined as the ratio of 100 V_f/V_i where V_i and V_f refer to the initial and final pellet, volume, respectively.

³Unconfined compressive strength of reduced pellets.

⁴The term r₄₀ was defined as the slope of curve (percent reduction with time) at 40-pct reduction according to equation 10.

⁵The terms t₉₀ and t_{max} refer to the time for 90-pct reduction and maximum weight loss, respectively.

⁶The total times for the 1,000° to 1,100° C reduction were 120 and 360 min, respectively.

Good agreement was obtained between the calculated and the experimental rates for all gas mixtures, except for 100 pct CH_4 at $1,100^\circ\text{C}$, where the calculated k_c was considerably lower than the experimental k_e (table 3 and figure 10). This deviation is probably due to complex CH_4 reactions occurring at this temperature. For example, the products (CO_2 and water vapor) from reduction can react with CH_4 to produce H_2 and CO , or CH_4 can be decomposed to H_2 and carbon.

The temperature dependence of the reaction rate in the range of 800° to $1,100^\circ\text{C}$ was also determined with the complex gas mixtures. The activation energies for L-Btu, M-Btu, RF-1, RF-2, and RF-3 were 15.5, 10.5, 12.6, 13.8, and 15.2 kcal/mol, respectively. The activation energies were similar to the values found for 100 pct H_2 and CO (fig. 4). This was

expected since the methane concentrations were low in the complex gas mixtures.

Other methods for determining the relative reduction kinetics were also used rather than the specific rate constant in equation 10. One of these methods was based on the time required to reach 90-pct reduction, and these data are shown in the bar graph in figure 11. These relative reduction data are in agreement with the earlier results, which showed that the H_2 content in the complex gases (table 1) and the temperature were the two most important variables affecting the reduction kinetics. These data also show that the time required for 90-pct reduction for simulated low-Btu gas is about the same as for 100 pct CO , but that the effectiveness of medium-Btu coal gas is between that of 100 pct CO and the reformed natural gases (RF-1 to RF-3).

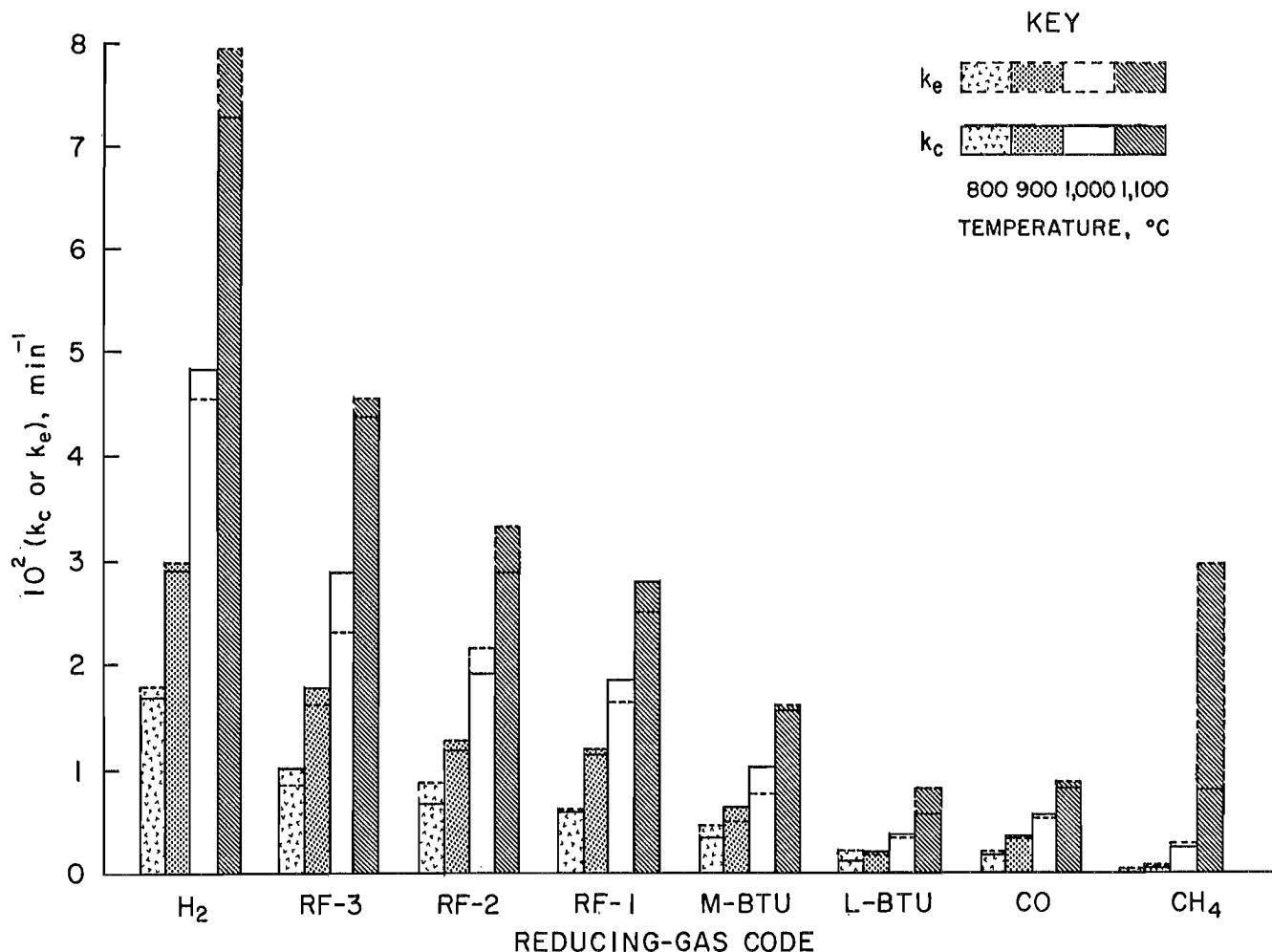


FIGURE 10. - Dependence of calculated and experimental reduction rate constants on gas composition and temperature.

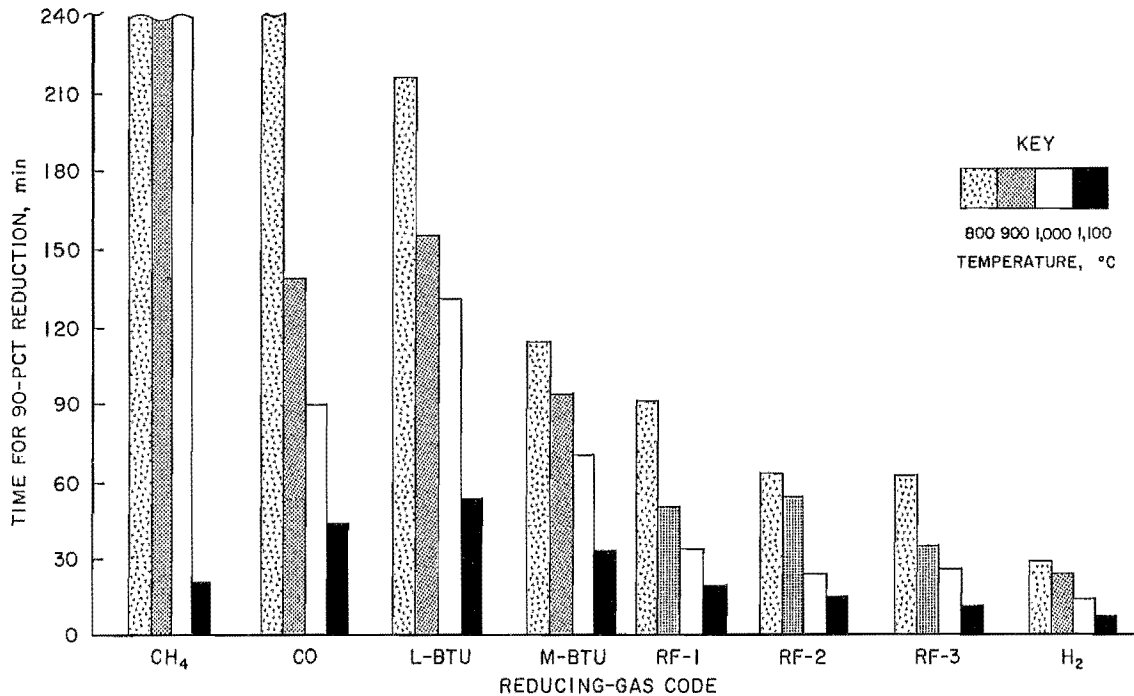


FIGURE 11. - Dependence of the 90-pct reduction time on type of reducing gas and temperature.

Another method (9) was also used to compare the relative reduction kinetics, which involves the slope of reduction-time curve at the 40-pct reduction (r_{40}) as determined by equation 10:

$$r_{40} = \frac{33.6}{(t_{60} - t_{30})}, \quad (10)$$

where t_{60} and t_{30} refer to time in minutes to obtain 60- and 30-pct reduction, respectively. The r_{40} values in table 3 were in agreement with the results discussed earlier, which showed the strong dependence of the reduction rate on temperature and H₂ content of the gas. Similar relative reduction observations were made by comparing the time required for maximum weight loss and 90-pct metallization (table 3). However, these two methods were not as good as the r_{40} method because 90-pct metallization and maximum weight loss were not reached in some cases. For example, a test using 100 pct CH₄ at 800° C did not meet these criteria even after 350 min.

EVALUATION OF REDUCED PELLETS

Chemical and physical properties of the pellets reduced with the different gas

mixtures are shown in table 3. More residual oxygen was retained in the pellet at the lower temperatures for the same reduction time, as shown by the percent metallization ($100 \text{ Fe}^{\circ}/\text{Fe}_T$). The percent carbon was the greatest with the CH₄- and CO-rich gases at the lowest temperatures. With 100 pct CO (or CH₄), the reduced pellets were black, rather than the normal gray, and had low compressive strengths. Earlier research in the Bureau's Twin Cities laboratory showed that the black coating was carbide and elemental carbon (5). Mazhenov (14) also reported the deposition of carbon when 100 pct CH₄ was used. The pellets that contained high carbon (over 10 pct) also had high swelling values.

The porosity of the pellets was determined before and after reduction. The results shown in figure 12 indicated that the pore volume with the reduced pellets was considerably greater than with the indurated iron oxide pellets before reduction. The total porosity of the reduced pellets was over 40 pct, while that of the oxide pellets was 21 pct. The pellets reduced with 100 pct H₂ appeared to have more micropores (i.e., 1.5 μm) than those reduced with 100 pct CO or low-Btu gas. This possibly can be

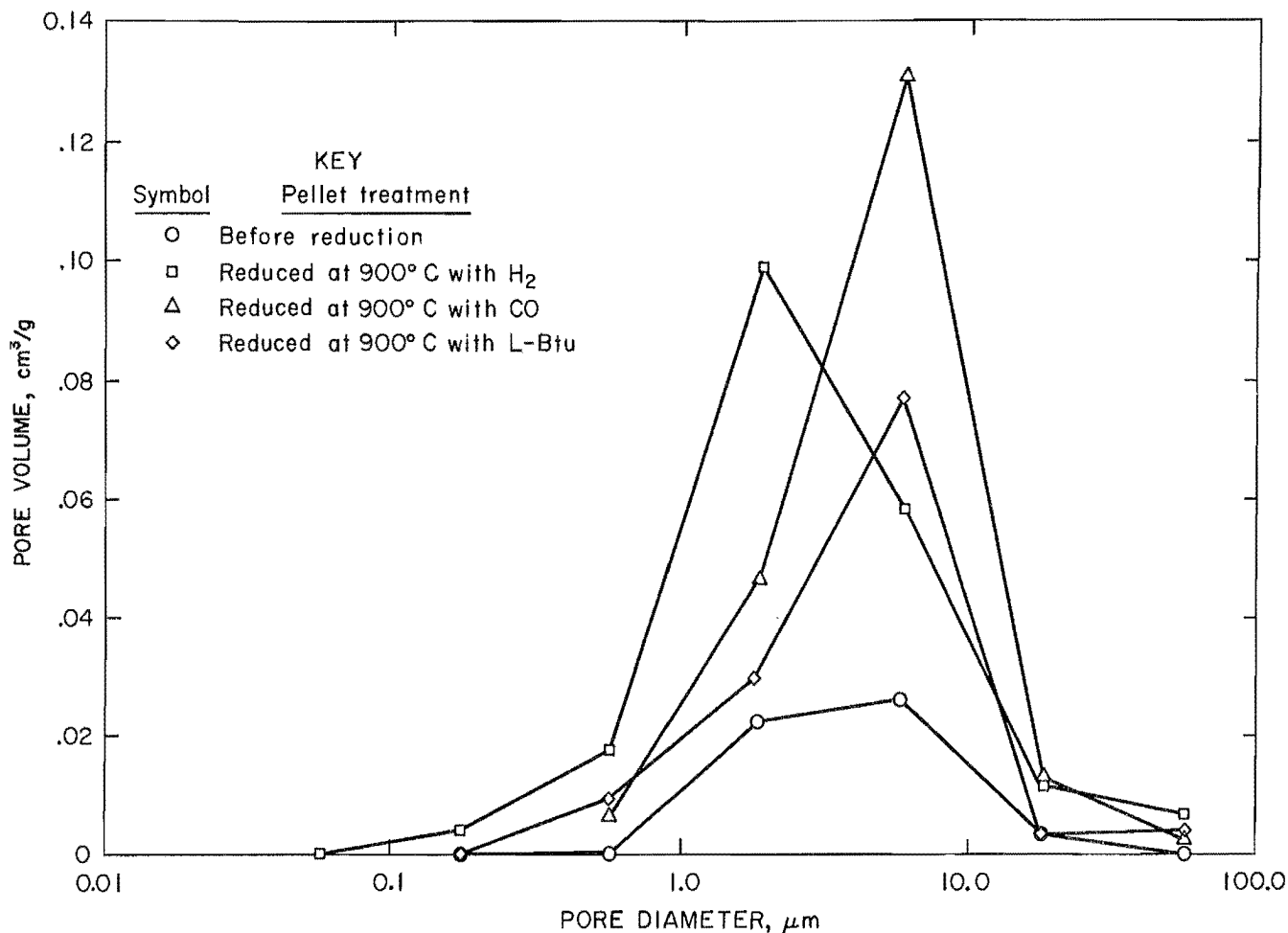


FIGURE 12. - Pellet pore size distribution before and after reduction.

explained by carbon deposition being favored with rich carbon monoxide gases and the elemental carbon plugging up the pores. Microscopic examination of the iron layer surrounding the residual iron oxide core indicated that the iron was very porous. Therefore, one

would suspect that mass transfer through the product layer was not the rate-controlling mechanism. This supports the earlier finding that a better fit was obtained with the topochemical rate equation (eq. 2) than with the gas diffusion equation (eq. 3).

CONCLUSIONS

This comparative study showed that the relative reduction rates are extremely dependent on the composition and temperature of the simulated coal gas. A semi-empirical model was developed to correlate the gas composition and temperature with the specific reduction rates at a total gas pressure of 1 atm. The exponent for the H₂ partial pressure term in the rate equation was about twice those of CO. Water vapor did not decrease the reduction rate as much as did CO₂. At

low temperatures, all reductants contributed significantly to the reduction rate except CH₄, which did so only at a high temperature (1,100° C). The time required to obtain 90-pct reduction with the low-Btu gas mixture was slightly longer than with 100 pct CO. With medium-Btu gas, less time was required than with 100 pct CO, but more time was required than with reformed natural gas or 100 pct H₂. The temperatures required to reach 90-pct reduction in about 1 h

with different gas mixtures were 800° C for 100 pct H₂, 800° C for RF-3, 900° C for RF-1 and -2, 1,000° C for M-Btu, and 1,100° C for L-Btu, 100 pct CO, and 100 pct CH₄. Carbon deposition was most noticeable with the rich CO gases at 800° C and with rich CH₄ gases at all

temperatures. At 900° C, over 90 pct of the iron oxide was reduced to iron in less than 3 h with low-Btu gas. This compares to a reduction time of 1.5 h with medium-Btu gas and 1 h with reformed natural gases.

REFERENCES

1. Al-Kahtany, M. M., and Y. K. Rao. Reduction of Magnetite With Hydrogen: Part I - Intrinsic Kinetics. *Ironmaking and Steelmaking*, v. 7, No. 2, 1980, pp. 49-58.
2. Ashworth, R. A., K. C. Yvas, and D. G. Bonamer. Study of Low and Intermediate Btu Gas From Coal for Iron Ore Pelletizing (contract J0255021, Arthur G. McKee & Co.). BuMines OFR 36-77, 1977, 214 pp.; NTIS PB 264702.
3. Bjorkvall, B., and G. Thaning. Test Methods for Agglomerated Products - Part I. *Scand. J. Metall.*, v. 1, 1972, pp. 57-58.
4. Guseman, J. R. Fuels and Reductants. Ch. in *Direct Reduced Iron Technology and Economics of Production and Use*, ed. by R. L. Stephenson. *Iron and Steel Soc.*, AIME, 1980, pp. 49-63.
5. Haas, L. A., S. E. Khalafalla, and P. L. Weston, Jr. Kinetics of Formation of Carbon Dioxide and Carbon From Carbon Monoxide in the Presence of Iron Pellets. BuMines RI 7064, 1968, 29 pp.
6. Hansen, J. P., J. E. Berryhill, and J. A. Aufman. Batch Reduction of Iron Ore in Fluidized Bed. BuMines RI 7461, 1970, 25 pp.
7. Hansen, J. P., T. N. Rushton, and S. E. Khalafalla. Reduction of Ferrous Oxide (Wustite) at High Temperature. BuMines RI 6712, 1966, 25 pp.
8. Hansen, J. P., T. N. Rushton, and C. W. Schultz. Reaction Interface Speed as a Reducibility Index for Iron Ore. BuMines RI 6827, 1966, 33 pp.
9. International Organization for Standardization. *Iron Ores--Determination of Reducibility*. ISO/DIS 4695, 1982, 8 pp.
10. Jackson, K. A. Metallized Pellets by the Hyl Process. *Proc. Annu. AIME Meeting, MN Sec., Duluth, MN, Jan. 15-17, 1973*, pp. 88-93.
11. Joyce, E. L., Jr., and K. Li. Reduction of Iron Ore Pellets in Simulated Low-Btu Gases. *Trans. Iron and Steel Soc. AIME*, Nov. 1984, pp. 61-64.
12. Kawai, M., H. Kimura, and T. Teramine. Reduction of Fine Iron Oxide by Carbon Monoxide, Hydrogen, and C₃H₈ Cracking Gas. *Tetsu to Hagane*, v. 46, No. 10, 1960, pp. 1130-32; *Chem. Abstr.*, v. 61: 1166 2C.
13. Kurzina, T. P., and S. E. Filippov. Kinetics of the Reduction of Iron Oxides by Mixtures of Carbon Monoxide and Hydrogen. *Izv. Vyssh. Uchebn. Zaved. Chern. Metall.*, v. 6, No. 9, 1963, pp. 5-10; *Chem. Abstr.*, v. 60: 2573 b.
14. Mazhenov, M. A., D. I. Ryzhonkov, V. F. Knybsev, and S. I. Filippov. Kinetic Reduction Characteristics of Pelletized Iron Ore Carried Out by Means of Hydrogen and Methane. *Izv. Vyssh. Uchebn. Zaved. Chern. Metall.*, v. 8, No. 7, 1965, pp. 11-15; *Chem. Abstr.*, v. 63: 9526 c.
15. McKewan, W. M. Kinetics of Iron Oxide Reduction. *Trans. Metall. Soc. AIME*, v. 218, No. 2, 1960, pp. 2-6.
16. Nigro, J. C. Firing an Iron Ore Pelletizing Kiln With Low-Btu Gas From Lignite. BuMines RI 8670, 1982, 22 pp.
17. Nigro, J. C., T. D. Tiermann, and C. Prasky. Kinetics of CO Reduction of Hematite to Magnetite and Effect of Silica. BuMines RI 7720, 1973, 43 pp.
18. Nigro, J. C., R. K. Zahl, and C. Prasky. Effect of Dolomitic Lime on Magnetite Taconite Pellets. *Trans. Soc. Metall. Eng. AIME*, v. 254, 1973, pp. 328-336.
19. Turkdogan, E. T., and J. V. Vinters. Gaseous Reduction of Iron Oxides, Part III Reduction - Oxidation of Porous and Dense Iron Oxides and Iron. *Metall. Trans.*, v. 3, 1972, pp. 1561-1574.